



Diffusion bonding beryllium to Reduced Activation Ferritic Martensitic steel: Development of processes and techniques

R.M. Hunt^{a,*}, S.H. Goods^b, A. Ying^a, C.K. Dorn^c, M. Abdou^a

^a Mechanical and Aerospace Engineering Department, UCLA, 44-128 Engineering IV, 420 Westwood Plaza, Los Angeles, CA 90025-1597, USA

^b Sandia National Laboratories, USA

^c Materion Brush Beryllium and Composites, USA

ARTICLE INFO

Article history:

Received 20 December 2011

Received in revised form 23 March 2012

Accepted 4 April 2012

Available online 26 April 2012

Keywords:

Beryllium

F82H

Diffusion

Bonding

HIP

Intermetallic

ABSTRACT

Beryllium was successfully bonded to a Reduced Activation Ferritic Martensitic (RAFM) steel with a maximum strength of 150 MPa in tension and 168 MPa in shear. These strengths were achieved using Hot Isostatic Pressing (HIP), at temperatures between 700 °C and 750 °C for 2 h and under a pressure of 103 MPa. To obtain these strengths, 10 μm of titanium and 20 μm of copper were deposited on the beryllium substrate prior to HIP bonding. The copper film acted a bonding aid to the RAFM steel, while the titanium acted as a diffusion barrier between the copper and the beryllium, suppressing the formation of brittle intermetallics that are known to compromise mechanical performance. Slow cooling from the peak HIP temperature along with an imposed hold time at 450 °C further enhanced the final mechanical strength of the bond.

© 2012 Elsevier B.V. All rights reserved.

1. Introduction

Fusion first walls experience high thermal and particle loads, which necessitate an armor layer to cover plasma-facing components. For such applications, beryllium is a prime candidate material, along with tungsten and carbon–carbon composites [1]. Beryllium is an advantageous armor material because it has a low atomic number, high thermal conductivity, low tritium retention, and low activation properties. This armor layer is meant to cover the first wall components, which will be constructed using Reduced Activation Ferritic Martensitic (RAFM) steel. One method of joining the armor to RAFM steel is HIP bonding, a solid state joining process by which interdiffusion of atoms is encouraged from one material into a closely pressed neighboring material to create a bond. The interdiffusion of materials creates a mixture of both materials at the joint interface, creating a metallurgically strong joint. Despite beryllium's advantages as an armor layer, there are three main limitations associated with bonding beryllium to RAFM steel that must be managed in order to create a robust joint. These

include incidental material annealing, thermal stress, and formation of intermetallic compounds.

For every material couple, there exists a bonding temperature threshold, below which atomic diffusion is insufficient to create a metallurgical bond. However, the bond temperature cannot be too high either, because higher temperatures increase the amount of incidental heat treatment done on the substrate materials. These constraints define a narrow design window for diffusion bonding beryllium to RAFM steel. Above 1000 °C, F82H (a qualified grade of RAFM steel used for this work) undergoes significant grain coarsening [2]. Additionally, beryllium shows grain coarsening above roughly 850 °C [3]. Also, post-weld heat treatments for F82H are meant to occur at only 720 °C [4,5]. Any HIP cycles significantly above these temperatures can potentially cause undesirable effects in F82H welds or in either bulk material.

The second major challenge of diffusion bonding is the creation of thermal stress that occurs as a product of differential thermal expansion of the joining materials. At room temperature, beryllium's thermal expansion coefficient is 11.6 μm/K, while F82H's is 10.4 μm/K. When the two materials are joined at a high temperature, the volumes are stress free. However, as the system cools to room temperature, beryllium shrinks at a faster rate than F82H, creating a complex stress profile throughout the system, including a global bending moment and a severe stress discontinuity at the interface. The resulting stress profile contains high shear and normal stresses that gather near the free edges of the bond, and are

* Corresponding author at: Lawrence Livermore National Laboratory, USA. Tel.: +1 310 893 9117; fax: +1 310 825 2599.

E-mail addresses: hunt52@llnl.gov (R.M. Hunt), shgoods@sandia.gov (S.H. Goods), ying@fusion.ucla.edu (A. Ying), christopher.dorn@materion.com (C.K. Dorn), abdou@fusion.ucla.edu (M. Abdou).

the driving forces for cracking and delamination of the interface [6–8].

Exacerbating the stress problem is the presence of intermetallic compounds formed during HIP bonding. These layers form when the interdiffusing elements have a lower energy state as a single-phase compound than they would as a two-phase mixture [9]. Beryllium is especially reactive to nearly all of the elements in the periodic table, forming compounds with much generally less desirable mechanical properties than the substrate materials. Specifically, these compounds are usually very brittle, and are therefore often the location of failure in a diffusion bond [1,10].

To counter the thermal stress from differential expansion, a copper interlayer was added between beryllium and ferritic steel substrates. This ductile layer absorbs some of the strain energy as plasticity instead of allowing that energy to cause fracture in the intermetallics [11,12]. However, diffusion-bonding copper between beryllium and ferritic steel has the unfortunate side effect of introducing beryllium–copper intermetallics, which are known to be especially brittle [13,14]. To resolve this, a thin titanium diffusion barrier was deposited between copper and beryllium such that the ductile compliance layer could be present without adverse beryllium–copper embrittlement [15]. Titanium has shown less affinity towards beryllium intermetallic formation, while beryllium diffuses relatively slowly through titanium, making titanium an excellent diffusion barrier choice for this application [16,13].

2. Procedures and methods

The formation of intermetallic compounds at the joint interface appears to be an unavoidable side effect of HIP bonding beryllium to another substrate [17,18]. As such, this study attempts to show that beryllium can be joined to RAFM steel if the brittle quality of the beryllium intermetallics can be managed. One hypothesized strategy to improve the quality of the joint is to include a ductile interlayer between beryllium and RAFM steel, which will plastically deform to absorb the strain energy produced from differential expansion. Numerical simulations were performed to show the role that a copper interlayer has on stress reduction near the interface. Following this, an experimental test campaign was conducted to join coupons of beryllium and RAFM steel under various combination of interlayers and bonding conditions. These techniques aim to maintain ductility in regions between each of the brittle intermetallic layers to create a more robust joint.

2.1. Numerical method

Abaqus 6.10, a commercial finite element software, was used to model the residual stress that is created near the beryllium to ferritic steel interface after diffusion bonding at high temperature. In the model depicted in Fig. 1, a 50-mm diameter cylinder was partitioned horizontally to delineate the diffusion bond. For analyses that included thin interlayers, multiple horizontal partitions defined the material thicknesses. In these simulations, the bond was modeled with axisymmetric geometry, utilizing linear 4-node elements (Abaqus number CAX4). The 2D axisymmetry model was constrained for symmetry at the axis, and axially at the base of the cylinder. The geometry was meshed with high mesh-bias towards both the material interface and the free edge of the sample, with a minimum element size of $1\ \mu\text{m} \times 1\ \mu\text{m}$.

With an initial uniform temperature of 700°C , a uniform temperature drop was applied to the system to simulate cooling to room temperature from the HIP bonding temperature. Temperature-dependent elastic–plastic behavior was included in the material property definitions of all materials [19–22]. The residual stress was modeled both as a steady-state and a

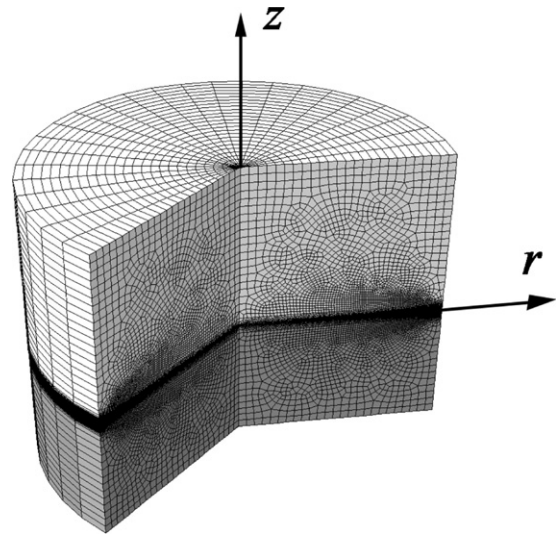


Fig. 1. Be/F82H bond was modeled with axisymmetric geometry, with a biased mesh towards the interface and free edges.

transient simulation; the steady state solution provided the time-independent residual stress after cooling, while the transient models portrayed the development of stress and strain during the cooling process. Additionally, time-dependent creep strain was included in the copper material definition to model the effect of different cooling schemes on the final residual stress [23].

2.2. Materials

For HIP bonding beryllium to ferritic steel, six 48-mm diameter cylinders of Beryllium S-65, Revision E (21.25 mm thick) and RAFM steel, F82H (15 mm thick) were machined. These were polished to a 400 nm finish with no more than 0.04% deviation in flatness. Fig. 2 displays the HIP can contents while Table 1 describes the material compositions.

On the bonding surface of the beryllium, two thin films were deposited via Plasma Vapor Deposition (PVD): 99.99% pure titanium, followed by 99.99% pure copper. Extremely high quality vacuum and sputter target were imperative, else contamination resulted in oxide formation in the deposition layers.

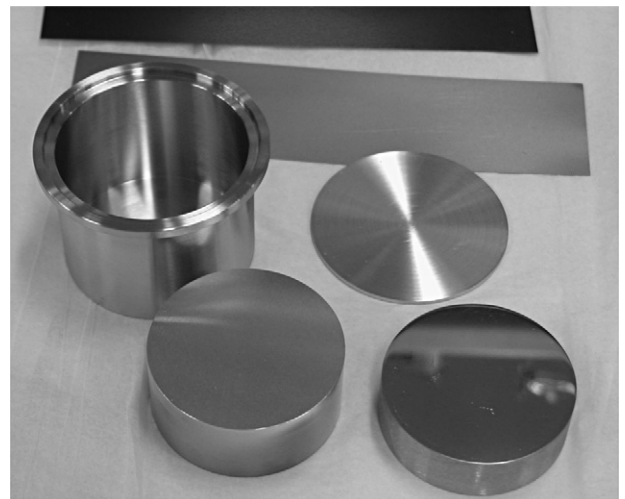


Fig. 2. Contents of the HIP can, clockwise from upper left: stainless steel HIP can, two rectangular shims, HIP can lid, F82H substrate, beryllium substrate.

Table 1
Chemical composition of F82H [2] and Be S65, Rev.E [3] (wt%).

	C	Si	Mn	S	Cr	W	V	Ta	Ti	N
F82H-IEA	0.090	0.07	0.10	0.001	7.82	1.98	0.19	0.04	0.004	0.007
Be S65, Rev.E	Be	BeO	Al	C	Fe	Mg	Si	Other		
	99.0	1.0	0.06	0.10	0.08	0.06	0.06	0.04		

Following polish and PVD, the surfaces were chemically cleaned to prepare them for joining. The ground ferritic steel was caustic cleaned in Oakite 90™ at 70 °C to remove oils and greases, rinsed in de-ionized water, isopropyl alcohol and blown dry with dry N₂ gas. The deposited copper was solvent cleaned with acetone, chemically polished in a mixture of nitric, phosphoric and acetic acids, and then rinsed and dried in the same fashion as the ferritic steel. This process was identical to that used in the ITER diffusion bonding processes to join CuCrZr to 316L stainless steel [24].

The prepared beryllium and RAFM samples were then encapsulated in a thin-walled (1.27 mm) stainless steel shroud that deformed under the high pressure of a HIP chamber to apply isotropic pressure around the substrates. The shroud was closed using an electron-beam weld while in vacuum. The HIP bonding process was performed at two temperatures, 700 °C and 750 °C, for 2 h at a pressure of 103 MPa. These conditions were determined through previous experimentation, which showed that copper does not bond well to ferritic steel for temperatures less than 700 °C (for a 2-h hold time) [25].

After the high temperature hold, two different cooling schemes were utilized. In one case, the chamber heater was completely shut off, allowing the samples to cool rapidly to room temperature. The other scheme cooled the sample at a controlled rate of 250 °C/h until 450 °C, where the sample was held for 4 h before being allowed to air cool (see Fig. 3).

2.3. Experimental parameters

Beryllium to ferritic steel bonds were fabricated under six different bonding conditions (as described in Table 2), creating four separate controlled experiments. Test 1 compared a direct bond (without interlayers) to a similar bond with copper–titanium interlayers, both bonded at 700 °C for 2 h. Test 2 showed the difference between a sample cooled by convection, and a sample cooled at 250 °C/h until a 4-h hold step at 450 °C, as depicted in Fig. 3. Test 3 studied the effect of HIP temperature, bonding at temperatures of 700 °C, 725 °C, and 750 °C for 2 h. The selection of these temperatures was guided by the results of previous work [25]. Finally, Test 4 demonstrated the effect of a thinner titanium diffusion barrier, from 10 μm down to 5 μm. In summary, the following four tests were conducted:

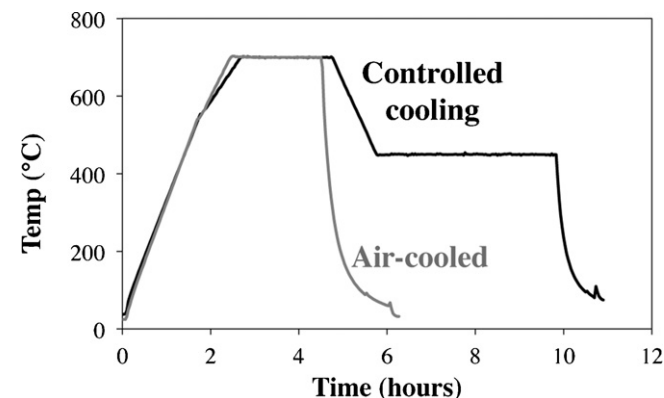


Fig. 3. HIP bonding temperature profiles under two cooling schemes.

- Test 1 Bond samples with and without metals interlayers.
- Test 2 Vary cooling scheme after bonding.
- Test 3 Vary bonding temperature: 700 °C, 725 °C, and 750 °C.
- Test 4 Vary titanium deposition thickness: 10 μm and 5 μm.

2.4. Characterization technique

After HIP bonding, specimens from each sample were extracted via electrical discharge machining for mechanical testing, micrography, and spectroscopy. The shear test specimen design was based on a modified DIN 50162/ASTM A263 standard, originally designed to measure the strength of a beryllium to copper interface. The specimens were mounted using a fixture that provided lateral support while loading the beryllium in pure shear akin to the aforementioned standards. The tensile specimens were of a simple, flat, dog-bone design, measuring 0.125 in. thick × 0.2 in. wide × 0.286 in. gauge length. Tests were performed on a SATEC Model 22EMP electromechanical test frame.

In order to characterize interdiffusion across the bondline, depth profiling was conducted on a scanning electron microscope (SEM) via energy dispersive and wavelength dispersive spectroscopy (EDS and WDS). This technique had the benefit of being sensitive to beryllium composition. The main drawback of this analysis technique was that no quantitative results were taken for atomic concentration in EDS or WDS. Instead, the X-ray counts of each element were normalized against the peak value obtained in the pure material regions. This gave qualitative comparisons for the relative amounts present in each intermetallic layer.

3. Results and discussion

This section discusses the findings of both the numerical simulations as well as the bonding experiments. Finite element analyses served to guide the design of the beryllium to RAFM steel joint by determining optimum parameters for the ductile interlayer. In this way, interlayer material properties, interlayer thickness, and cooling scheme were refined prior to beginning the experiment. Though interface composition and strength are covered sequentially, they are interconnected, as differences in composition are the basis for joint strength. Since intermetallics are often the source for brittle fracture in diffusion bonds, this section will first catalog exactly how and where they form under different bonding conditions. This will be followed by a discussion of the effects of the different bonding variables on joint tensile and shear strengths.

3.1. Numerical results

Inserting a 20 μm thick copper layer between beryllium and ferritic steel significantly reduced radial and shear residual stress (see Fig. 4). In a model where the substrates were cooled from 700 °C down to room temperature, bonds without any interlayers generated high radial and shear stress near the material interface. At $r = 24$ mm (from the center axis) and $z = 20$ μm (into Be from the interface), $\sigma_{rr} = 158$ MPa and $\sigma_{rz} = -90$ MPa (gray lines in Fig. 4). In contrast, a similar analysis that included a 20 μm thick copper interlayer between substrates produced only $\sigma_{rr} = 46$ MPa and $\sigma_{rz} = -45$ MPa at the same location (black lines in Fig. 4). This equates to a 71% reduction in radial stress, and 50% reduction in

Table 2
Diffusion bonding experimental conditions and strength results.

Sample #	1	2	3	4	5	6
HIP temperature	700 °C	700 °C	700 °C	725 °C	750 °C	700 °C
Hold step temperature	450 °C	–	450 °C	450 °C	450 °C	450 °C
Ti thickness	–	10 μm	10 μm	10 μm	10 μm	5 μm
Cu thickness	–	20 μm	20 μm	20 μm	20 μm	20 μm
Avg. tensile strength	debond	45 MPa	131 MPa	174 MPa	171 MPa	82 MPa
Avg. shear strength	debond	debond	169 MPa	168 MPa	167 MPa	180 MPa

shear. The F82H substrate saw a similar beneficial stress reduction with the additional copper layer.

Increasing the thickness of the copper interlayer produced little additional stress reduction. Performing the same analysis as above with 40 μm thick and 10 μm copper interlayers produced nearly the same stress profiles as the 20 μm layer, indicating that thickness of the copper layer is not critical in this design. However, this stress reduction comes at the cost of high plastic strain in the copper, which may make copper subject to plastic rupture. This scenario can be modeled by comparing the copper plastic equivalent to its temperature-dependent rupture limit, following the equation:

$$\varepsilon = (1 \times 10^{-7})T^2 - (0.0004)T + 0.3108 \quad (1)$$

where T is in units of °C [19]. Since plastic stress and strain are highest close to the free edge, the elemental equivalent plastic strain was averaged over the last 100 μm of the copper to represent the highest strain region. This area included the edge stress singularity,

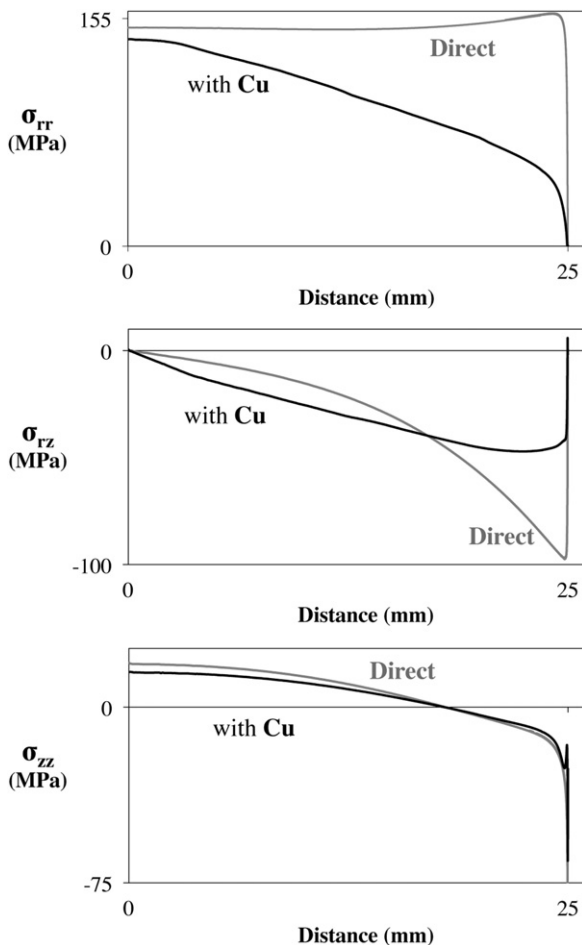


Fig. 4. Elastic-plastic component stress in the beryllium, 20 μm from the joint. Adding a 20 μm thick copper layer significantly reduced both radial and shear components close to the free edge.

which caused the average stress and strain to be over-estimated. The resulting comparison showed that a 10 μm thick copper layer exceeded plastic rupture during cool-down. A 20 μm copper layer only briefly exceeded the rupture limit, and a 40 μm was safe from rupture. Since the thicker interlayers are able to distribute strain over a thicker region, they are less likely to fail.

As shown in the static analysis above, a copper interlayer reduced stress near the edge of the sample by deforming plastically. However, in a simulation of a 2-h cool-down from 750 °C, strain in the copper plateaued at just above 20% total strain, long before the samples arrived at room temperature. The reason for this is that as the copper cooled, its yield limit increased, reducing the ability for copper to plastically deform. This is easiest to understand in Fig. 5, which depicts equivalent plastic strain versus Von Mises stress from the last 100 μm of the copper closest to the free edge. At 750 °C, plastic deformation occurred without significant stress increase. However, as temperature decreased, the copper material increased hardness, and more stress was required for further plastic deformation. As temperature cooled below 400 °C, the copper could not deform further without additional stress, which caused straining to occur in the beryllium and steel substrates. The conclusion from this is that copper is only effective as a compliant layer between 750 °C and 400 °C; below 400 °C, the copper is not helping to reduce stress in either the beryllium or RAFM steel.

Since copper has a melting point that is considerably lower than titanium, beryllium and RAFM steel, it undergoes far more creep strain than the other materials during the cool-down from fabrication. For this reason, in time-dependent analyses, beryllium and RAFM steel were treated as elastic substrates, while the copper interlayer was considered to have time-dependent creep properties. The effect of creep strain on surrounding substrates was determined for three different cooling schemes: air-cooled, linear-cooled, and cooled with an intermediate hold step. To compare stress results from the different cooling regimes, data were averaged from a 100 μm × 20 μm rectangle at the corner of the interface and the free edge. This area contained the highest stress results, and averaging the data reduced the effect of the edge stress singularity.

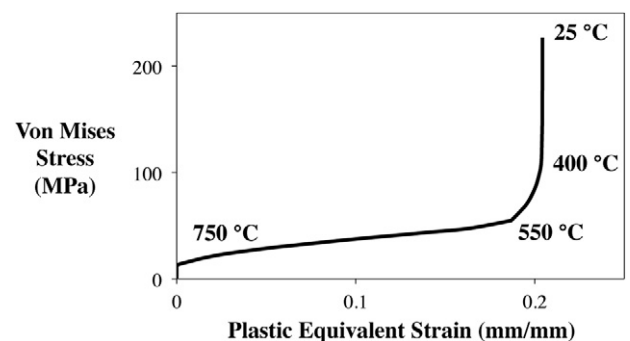


Fig. 5. As copper hardens, it loses its ability to plastically strain under low stress. As a result, below 400 °C, copper is not as effective as a means of reducing stress in the surrounding substrates.

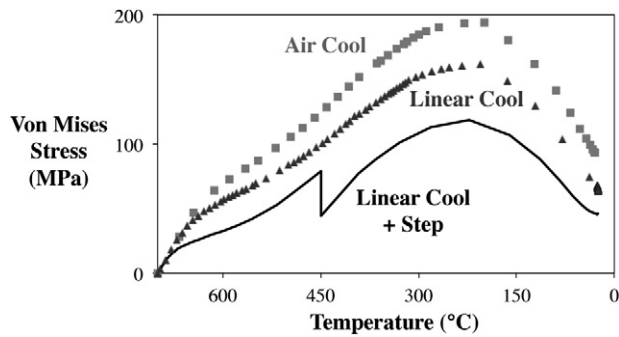


Fig. 6. Modeling the time-dependent creep of copper showed that reducing cooling rate and adding a hold step can significantly reduce Von Mises stress in the beryllium.

The first cooling scheme simulated the condition in which a diffusion bonded sample is subjected to room-temperature air immediately after bonding, and is cooled by convection. This scheme involved the fastest cooling rate, and produced a peak elastic Von Mises stress in the beryllium of 193 MPa and a final room-temperature residual stress of 93 MPa (light gray line in Fig. 6). The second cooling scheme reduced the temperature of the system at a 250 °C/h rate, and produced a peak stress in the beryllium of 162 MPa and a room-temperature stress of 68 MPa (dark gray line in Fig. 6). The last scheme cooled the system at the same linear rate, but also included an intermediate hold step at 450 °C for 4 h, producing a peak beryllium stress of 118 MPa and room-temperature stress of 45 MPa (black line in Fig. 6). Compared with the air-cooled scheme, this last cooling scheme reduced beryllium peak stress by 39% at peak, and room-temperature stress by 51%. Similarly, F82H peak stress was reduced 30% (from 161 MPa to 113 MPa) and room-temperature stress was reduced 35% (from 120 MPa to 78 MPa). Care should be taken not to place too much emphasis on the magnitude of values obtained, as these analyses are mainly for comparison to one another.

An interesting feature of the transient stress profiles in Fig. 6 are the peaks in stress that occur before the system comes to rest at room temperature. The stress profiles derive from differential thermal strain, which is the product of the difference of thermal expansion coefficients by the change in temperature:

$$\varepsilon_{th} = \Delta\alpha(T - T_i) \quad (2)$$

where ε_{th} is the thermal strain, $\Delta\alpha$ is the difference between the two materials' coefficients of thermal expansion, T is the final temperature, and T_i is the initial temperature. Generally, from this equation, the bigger the temperature drop, the bigger the strain. Interestingly, the peak stress during cooling did not occur at room temperature. Instead the stress in both beryllium and steel increased until 209 °C, and then began to decrease down to room temperature. This is due to the fact that the thermal expansion coefficients of beryllium and F82H are non-linear, and the greatest difference between them occurs at 209 °C.

3.2. Interface composition

The sample bonded without copper or titanium interlayers allowed interdiffusion of beryllium to occur directly with F82H steel. After a 2-h HIP hold at 700 °C, the resulting bond contained a 2.5 μm thick intermetallic compound between substrates. Fig. 7 shows a secondary electron micrograph of this interface, where beryllium and RAFM steel were identified via WDS and EDS, respectively. Determining the intermetallic phase at the interface was not possible using this measurement technique. In contrast, samples with deposited interlayers prevented formation of this Be–Fe compound, but formed both Be–Ti and Cu–Ti intermetallic compounds.

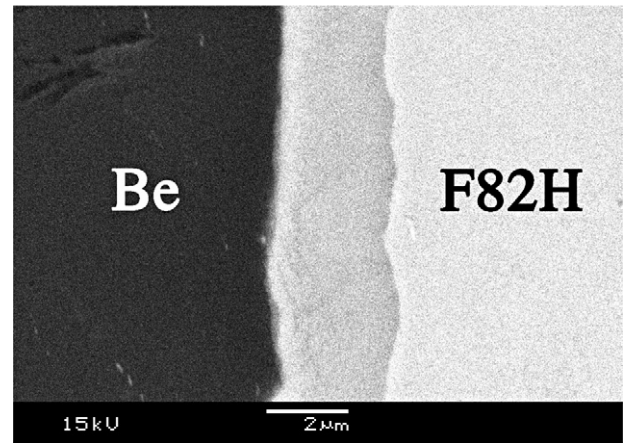


Fig. 7. Secondary electron image of a sample bonded at 700 °C for 2 h, without interlayers. A single, 2 μm-thick intermetallic formed between substrates.

Fig. 8 shows depth profile of one such sample that is typical of the redistribution of alloy constituents after HIP bonding. These interdiffusion regions will be discussed individually in this section.

At least two thin intermetallics formed at the beryllium–titanium interface during bonding. Fig. 9a shows how, after a HIP bond of 750 °C for 2 h, the interface between beryllium and one phase of Be–Ti remained nearly planar, while the rest of the Be–Ti phases diffused in a clearly non-planar fashion. Interestingly, there are no single-phase compounds in the beryllium–titanium binary phase diagram, and as such, these phases were not immediately identified. The thickness of this interdiffusion region grew from slightly less than 2 μm after a 700 °C HIP up to almost 5 μm after a 750 °C HIP.

Two copper–titanium intermetallics were dominant at the Cu–Ti interface for all bonding conditions. Fig. 9b shows the interface after a 725 °C HIP bond, with two such intermetallics. According to the copper–titanium binary phase diagram, two single-phase compounds exist: Cu₄Ti and CuTi. Correspondingly, at the Cu–Ti interface, EDS and WDS revealed two clear composition plateaus very close to the atomic ratios of Cu₄Ti and CuTi: one with average concentrations of 74.8% Cu and 19.2% Ti, and the other with 44.4% Cu and 45.2% Ti. Both compounds were of similar thickness, and grew with respect to increasing HIP temperature. Each phase was 3 μm thick for a HIP at 700 °C, 4–5 μm thick for a HIP at 725 °C, and 6 μm for a 750 °C HIP bond.

The copper–steel interface did not produce any intermetallics whatsoever, irrespective of bonding conditions. Fig. 9c shows the interface after a 700 °C bond, and higher temperature bonds equally produced little to no intermetallics. The far right of Fig. 8 shows how

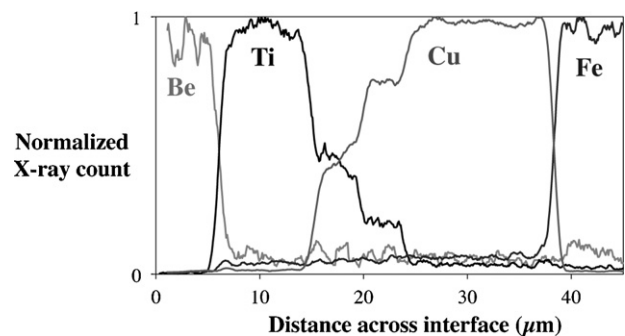


Fig. 8. EDS line trace (with WDS to capture beryllium signal) of a sample bonded at 725 °C for 2 h, with 10 μm Ti and 20 μm Cu. Each element has been normalized by its peak X-ray count.

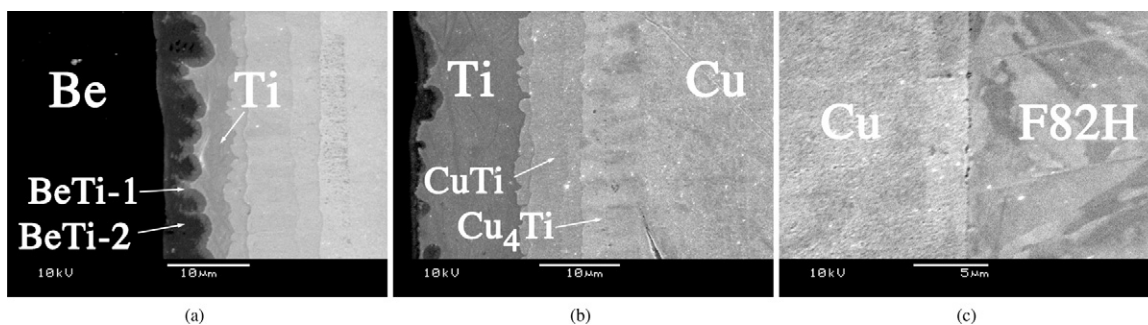


Fig. 9. Secondary electron images after HIP bonding of samples with both copper and titanium interlayer. (a) Beryllium/titanium interface after bonding at 750 °C. At least two intermetallic phases appeared at the Be/Ti interface, as indicated by the two distinct shades between Be and Ti. (b) Titanium/copper interface after bonding at 725 °C. Two thick intermetallic phases appeared at the Cu/Ti interface. (c) Copper/F82H interface after bonding at 700 °C. Cu and F82H did not form any significant intermetallic compounds.

little interdiffusion has occur at between copper and iron after a 725 °C HIP bond. This is in accordance with the copper–iron and copper–chromium phase diagrams, which indicate that at these bonding temperatures, copper and iron (as well as copper and chromium) do not form any single-phase compounds.

3.3. Strength characterization

When bonded without any metal interlayers, the beryllium to ferritic steel joint fractured prior to shear or tensile testing. Bonding was achieved in this joint, though the joint was unable to overcome the thermal residual stress due to cooling from fabrication temperature. Fig. 10 shows significant amounts of iron and beryllium on the beryllium side of the fracture plane, while only iron was present on the RAFM side of the fracture. This indicates that fracture occurred between the intermetallic and the RAFM steel. Lastly, the morphology of the exposed surface suggests brittle fracture, indicating that the two substrates were once mechanically joined.

As shown in the mechanical test results in Fig. 11 (HIP Test #2 and #3), samples that were cooled under a controlled scheme had almost three times the tensile strength of air-cooled samples (131 MPa compared to only 45 MPa). Additionally, controlling the rate of cooling changed the location of the fracture plane. Fig. 12a shows the exposed face of an air-cooled sample, which has fractured in the copper–titanium diffusion region, revealing both CuTi and Cu₄Ti intermetallics. In contrast, samples that underwent controlled cooling failed in the beryllium–titanium intermetallic region. Fig. 12b shows a fractured surface from this bonding

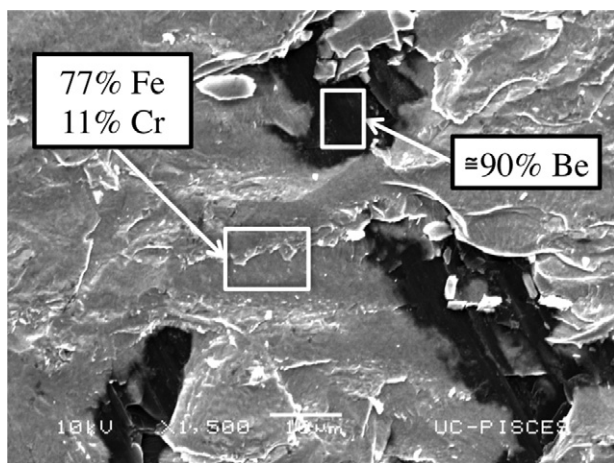


Fig. 10. Secondary electron image of the beryllium side of the tensile fracture surface of a sample bonded at 700 °C without interlayers. High concentrations of both iron and beryllium were present, suggesting fracture in the intermetallic.

condition, which exposes a titanium–beryllium plane (81% Ti, remainder Be) covered by small areas of high concentrations of beryllium (12% Ti, remainder Be).

The favorable cooling scheme had both a slower cooling rate and a hold step, making it difficult to determine if the cooling rate or the hold step played a greater role in stress reduction. Testing using additional cooling rates and different hold steps may be useful to differentiate these features and to determine the optimum cooling scheme for maximization of bond strength and toughness.

In Fig. 11, HIP Test #3, #4, and #5 show that joint strength was not drastically affected within a bond temperature range of 700–750 °C. The shear strength of each of these samples was roughly equivalent, with an average strength of 167 MPa. The tensile strength was only slightly improved with the increasing HIP temperature, from an average of 131 MPa after a 700 °C bond to 172 MPa for both the 725 °C and 750 °C HIP temperatures. The strengths of these samples were similar because the material composition across the interface was similar in all three cases. Most notably, all three cases contained enough titanium to prevent formation of Be–Cu. However, had copper penetrated through the titanium to interdiffuse with beryllium (e.g. if HIP temperatures exceeded 750 °C), the composition of the joint would have changed and likely resulted in a lower bond strength. These results indicate that any temperature between 700 °C and 750 °C (for a 2-h hold time) is appropriate.

The fracture plane of the tensile samples became more complex with higher HIP temperatures. For samples bonded at 700 °C, the crack stayed along the Be–Ti intermetallic almost exclusively. However, at higher HIP temperatures, the crack jumped back and forth between Be–Ti and Cu–Ti intermetallics, both of which were

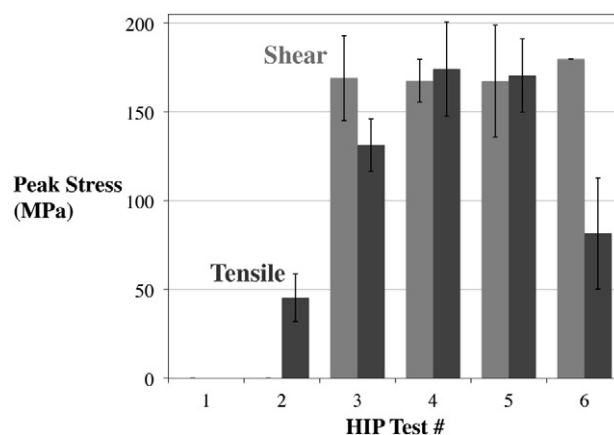
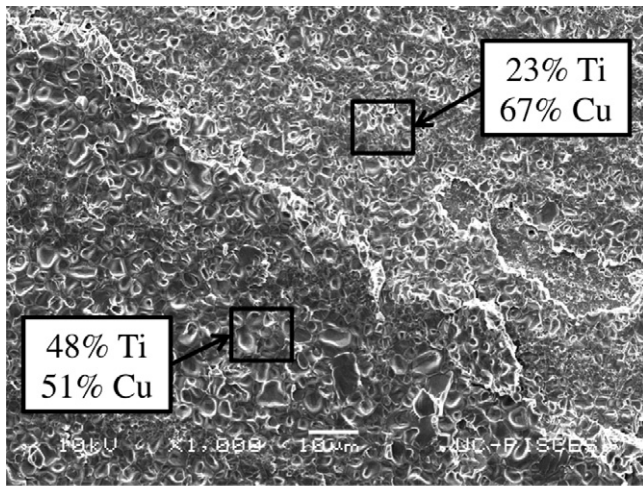
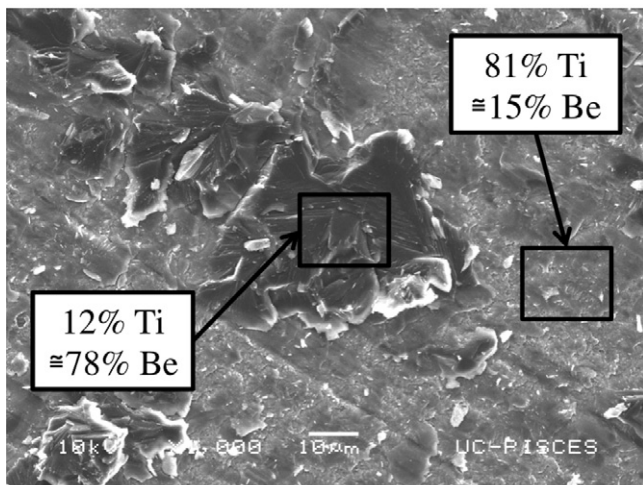


Fig. 11. Tensile and shear test results of bonded samples using six different bonding conditions (as described in Table 2).



(a) Sample cooled convectively from bonding temperature.



(b) Sample cooled at 250 °C/hour until a four hour hold at 450 °C.

Fig. 12. Tensile fracture surface in samples deposited with 10 μm Ti and 20 μm Cu and bonded at 700 °C. Reducing the cooling rate and adding a relaxation step moved the fracture plane from the Cu–Ti intermetallics in (a) to the Be–Ti intermetallics in (b).

brittle in comparison to the Be, Ti, and Cu. In the higher temperature HIP bonds, the titanium was thin enough to allow the crack to take advantage of weak sections (from voids or impurities) in either intermetallic, creating a more complex fracture (visualized in Fig. 13). It is unclear whether or not the Cu–Ti intermetallics

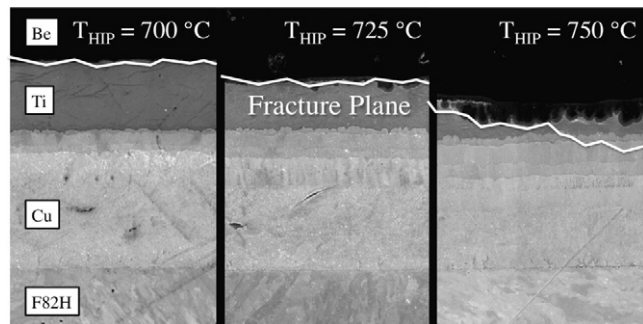


Fig. 13. Thinner titanium allowed the tensile fracture surface to jump between intermetallics to take the path of least resistance. All three secondary electron images are cross sections of samples that were initially deposited with 10 μm Ti and 20 μm Cu. The fracture plane depicted here is based on spectroscopy of individual fractured surfaces.

weakened relative to the Be–Ti intermetallics with increasing temperature, or if both intermetallics had similar strengths, and the depletion of titanium simply reduced ductility between two equally brittle layers.

Reducing the titanium film thickness to 5 μm had a similar effect on the fracture plane as did increasing the diffusion bonding temperature by 50 °C. Specifically, the thin amount of remaining titanium after interdiffusion allowed the crack to traverse from beryllium–titanium to copper–titanium intermetallics, resulting in a complex fracture plane. However, Fig. 11 shows that despite their fracture similarity, samples bonded at 700 °C with only 5 μm of titanium (#6) were 39% weaker (81 MPa instead of 131 MPa) in both shear and tensile than similarly bonded samples with 10 μm of titanium (#5).

4. Conclusions

A favorable set of conditions was determined to successfully bond beryllium to ferritic steel. The effectiveness of both the interlayers and the slow cooling scheme was confirmed, achieving a maximum joint strength of 153 MPa under tensile loading and 168 MPa under shear. These strengths were obtained with:

- Titanium thickness: 10 μm
- Copper thickness: 20 μm
- Bonding temperature: between 700 °C and 750 °C
- Intermediate hold during cooling: 4 h at 450 °C

In stark contrast, without these interlayers, the beryllium to ferritic steel joint debonded during cool-down from residual stress. Additionally, the addition of an intermediate hold step after a reduced cooling rate more than doubled the tensile strength of the joint. In all the cases that had an intermediate hold step, fracture occurred mainly in the Be–Ti intermetallic region. In addition, where the titanium layer was thin (when bonding temperature was higher or less titanium was deposited), the fracture plane was noticeably more complex, containing both Be–Ti and Ti–Cu intermetallics.

To further improve this joint, the beneficial aspects that were developed from a controlled cooling rate should be investigated further. It is possible that a longer intermediate hold step, or an ever slower cooling rate may yield further benefit. Since copper and steel are known to bond at strengths higher than 200 MPa [25], further investigations should focus on improvements to the intermetallic regions, as these regions were the limiting factors in the strength and ductility of the developed joint. Bonding experiments of titanium direct to copper (or beryllium direct to titanium) may be useful in this regard.

While this research is clearly most beneficial to work specific to beryllium joining technology, much of the findings can be utilized in the design of other dissimilar material joints. A copper interlayer would be particularly well suited to aid the joining of tungsten to ferritic steel, two materials with very different thermal expansion coefficients, due to copper's ability to effectively reduce residual stress. More importantly, copper is insoluble in both tungsten and iron and may aid in reducing thermal stress without forming any brittle intermetallic compounds, allowing creation of a joint that is both strong and ductile.

Acknowledgements

The authors would like to thank Brush Wellman Inc. (Elmore, OH), Bodycote (Andover, MA), Thin Film Technology Corp. (Buellton, CA), Axsys Technologies Inc. (Cullman, AL), and Electrofusion Products (Fremont, CA) for their contributions to this research,

without which this work would not have been possible. F82H was supplied by JAEA through the TITAN collaboration via Dr. Takuya Yamamoto (Dept. of Chemical Engineering, UCSB, Santa Barbara, CA).

Sandia is a multiprogram laboratory operated by Sandia Corporation, a Lockheed Martin Company, for the United States Department of Energy's National Nuclear Security Administration under contract DE-AC04-94AL85000.

References

- [1] B. Odegard Jr., C. Cadden, N. Yang, Beryllium–copper reactivity in an iter joining environment, *Fusion Engineering and Design* 41 (1998) 63–71.
- [2] T. Hirose, K. Shiba, T. Sawai, S. Jitsukawa, M. Akiba, Effects of heat treatment process for blanket fabrication on mechanical properties of F82H, *Journal of Nuclear Materials* 329 (2004) 324–327.
- [3] S-65 Structural Grade Beryllium Block, Brush Wellman Inc., revision c edition, 1987.
- [4] D. White, J. Burke, *The Metal Beryllium*, American Society for Metals, 1955.
- [5] T. Sawai, K. Shiba, A. Hishinuma, Microstructure of welded and thermal-aged low activation steel F82H IEA heat, *Journal of Nuclear Materials* 283 (2000) 657–661.
- [6] Y. Kin, T. Yamamoto, T. North, Generation and reduction of residual stress in ceramic/metal joints (mechanics, strength & structural design), *Transactions of JWRI* 21 (1992) 285–291.
- [7] A. Levy, Thermal residual stresses in ceramic-to-metal brazed joints, *Journal of the American Ceramic Society* 74 (1991) 2141–2147.
- [8] J. Blanchard, R. Watson, Residual stresses in bonded armor tiles for in-vessel fusion components* 1, *Nuclear Engineering and Design. Fusion* 4 (1986) 61–66.
- [9] P. He, D. Liu, Mechanism of forming interfacial intermetallic compounds at interface for solid state diffusion bonding of dissimilar materials, *Materials Science and Engineering: A* 437 (2006) 430–435.
- [10] M. Ghosh, K. Bhanumurthy, G. Kale, J. Krishnan, S. Chatterjee, Diffusion bonding of titanium to 304 stainless steel, *Journal of Nuclear Materials* 322 (2003) 235–241.
- [11] K. Saganuma, T. Okamoto, M. Koizlmi, M. Shimada, Effect of interlayers in ceramic-metal joints with thermal expansion mismatches, *Journal of the American Ceramic Society* 67 (1984) C–256.
- [12] T. Yamada, K. Yokoi, A. Kohno, Effect of residual stress on the strength of alumina-steel joint with Al–Si interlayer, *Journal of Materials Science* 25 (1990) 2188–2192.
- [13] V. Barabash, M. Akiba, A. Cardella, I. Mazul, B. Odegard Jr., L. Pl"ochl, R. Tivey, G. Vieider, Armor and heat sink materials joining technologies development for iter plasma facing components, *Journal of Nuclear Materials* 283 (2000) 1248–1252.
- [14] C. Cadden, B. Odegard Jnr, Aluminum-assisted joining of beryllium to copper for fusion applications, *Fusion Engineering and Design* 37 (1997) 287–298.
- [15] P. Sherlock, A. Erskine, P. Lorenzetto, A. Peacock, Application of a diffusion bonding methodology to develop a Be/Cu HIP bond suitable for the ITER blanket, *Fusion Engineering and Design* 66 (2003) 425–429.
- [16] T. Kuroda, T. Hatano, M. Enoda, S. Sato, K. Furuya, H. Takatsu, T. Iwadachi, K. Nishida, Development of joining technology for be/cu-alloy and be/ss by hip, *Journal of Nuclear Materials* 258 (1998) 258–264.
- [17] M. Enoda, M. Akiba, S. Tanaka, A. Shimizu, A. Hasegawa, S. Konishi, A. Kimura, A. Kohyama, A. Sagara, T. Muroga, Overview of design and R&D of test blankets in Japan, *Fusion Engineering and Design* 81 (2006) 415–424.
- [18] P. Zhang, B. Bai, L. Shen, J. Zhou, Distribution of the composition and micromechanical properties of Be/316L stainless steel following diffusion bonding, *Surface and Interface Analysis* 32 (2001) 88–90.
- [19] R. Carreker Jr., W. Hibbard Jr., Tensile deformation of high-purity copper as a function of temperature, strain rate, and grain size, *Acta Metallurgica* 1 (1953) 654–655.
- [20] S. Goods, D. Dombrowski, Mechanical properties of S-65C grade beryllium at elevated temperatures, Technical Report, Sandia National Labs., Livermore, CA (United States), 1997.
- [21] P. Spätig, G. Odette, E. Donahue, G. Lucas, Constitutive behavior and fracture toughness properties of the F82H ferritic/martensitic steel, *Journal of Nuclear Materials* 283 (2000) 721–726.
- [22] T. Leguey, N. Baluc, R. Schäublin, M. Victoria, Structure–mechanics relationships in proton irradiated pure titanium, *Journal of Nuclear Materials* 307 (2002) 696–700.
- [23] G. Li, B. Thomas, J. Stubbins, Modeling creep and fatigue of copper alloys, *Metallurgical and Materials Transactions A* 31 (2000) 2491–2502.
- [24] S. Goods, J. Puskar, Solid state bonding of cu/cr to 316l stainless steel for iter applications, *Fusion Engineering and Design* (2011).
- [25] R. Hunt, S. Goods, A. Ying, C. Dorn, M. Abdou, Evaluation of cu as an interlayer in be/f82h diffusion bonds for iter tbm, *Journal of Nuclear Materials* (2010).